Analyst

PAPER

View Article Online
View Journal

Cite this: DOI: 10.1039/c7an01498h

QCM-nanomagnetic beads biosensor for lead ion detection

Qingli Zhang,[a] Haixia Cui,[a] Xingliang Xiong,[a] Jun Chen,[b] Ying Wang,[c] Jia Shen,[a] Yiting Luo[a] and Longcong Chen *[a]

Received 9th September 2017,
Accepted 4th December 2017

DOI: 10.1039/c7an01498h

rsc.li/analyst

As lead poses a serious threat to humans even in small amounts, all kinds of lead detection sensors with high sensitivity and selectivity are being constantly improved and put forward. In this report, a novel, simple and label-free quartz crystal microbalance (QCM) biosensor is proposed for detecting lead ions (Pb^{2+}). The biosensor takes full advantage of the high specificity of GR-5 DNAzyme to Pb^{2+} and the high sensitivity of QCM. In particular, nanomagnetic beads (NMBs) are used as a novel and effective mean of signal amplification in the biosensor because of their mass and their ability to enhance the inductive effect, which are very beneficial for both higher sensitivity and a lower detection limit. In practice, GR-5 DNAzyme, innovatively combined with NMBs, was modified on the gold electrode of the QCM through gold–sulfur self-assembly. When the electrode was exposed to Pb^{2+} solution, DNAzyme was severed into two parts at the RNA site (rA), along with the release of NMBs, which caused a great increase in frequency shift of the QCM electrode. Finally, a perfect linear correlation between the logarithm of Pb^{2+} concentration and the change in frequency was obtained from 1 pM to 50 nM, with a detection limit as low as 0.3 pM. Moreover, the biosensor shows both an average recovery of 97 ± 6% in a drinking water sample and an excellent specificity for Pb^{2+} compared with other metal ions.

1. Introduction

As we all know, lead, a poisonous heavy metal, is ubiquitous in our daily lives. If even a tiny amount of Pb^{2+} is exposed, it can accumulate in the environment because of its non-biodegradable nature,[1] resulting in the pollution of drinking water and soil, bringing about a serious and long-lasting threat to human health and having a severe effect on children in particular.[2] Therefore, it is vital to design a simple, highly selective and sensitive method of Pb^{2+} monitoring for both human health and the environment.

The traditional detection methods for Pb^{2+} are mainly based on spectroscopy and mass spectrography,[3] such as atomic absorption spectrometry (AAS),[4] graphite furnace atomic absorption spectrometry (GFAAS)[5] and multiple collector inductively coupled plasma-mass spectrometry (MC-ICP-MS).[6] These methods can determine the concentration of Pb^{2+} precisely. In the meantime, we cannot ignore the disadvantages of long-running operation of samples, expensive cost, intricate equipment and highly qualified technicians.[7] Plenty of excellent efforts have been devoted to overcoming these limitations. In particular, DNA sensors are of great interest and have been widely used for gene analysis, medical analysis and environmental pollution monitoring due to their low cost, and high sensitivity and selectivity. DNAzyme-based biosensors, using various signal transducers to detect a wide range of metal ions, have drawn more and more attention among researchers. To the best of our knowledge, Pb^{2+}-dependent DNAzymes, such as GR-5 and 8–17 DNAzyme are widely utilized in Pb^{2+} detection with colorimetric,[8,9] fluorescent,[10–12] and electrochemical[13–16] signal readouts as the sensing signals. And recently, Lu *et al.*[17] reported that GR-5 DNAzyme shows a higher selectivity for Pb^{2+} than 8–17 DNAzyme. Colorimetric-based biosensors have attracted increasing interest due to their merits of simplicity and cost-effectiveness.[18] Investigators have presented colorimetric methods based on the self-assembly of gold nanoparticles (AuNPs) with glutathione (GSH) or DNA strands as linkers.[2,19] In previous work, our group designed a colorimetric method for the determination of Pb^{2+}, which was based on the different adsorption capacities on the surface of AuNPs between ssDNA (single-stranded DNA) and the G-quartet.[20] However, colorimetric sensors suffer from an unsatisfactory detection limit for Pb^{2+}. Compared with these biosensors, fluorescent-dependant methods show a higher sensitivity, but fluorophores and/or quenchers are necessary in fluorescent

[a]Department of Biomedical Engineering, Chongqing Medical University, Chongqing, 400010, China. E-mail: clc_mpd@163.com
[b]School of Public Health and Management, Chongqing Medical University, Chongqing, 400010, China
[c]School of Medical Information Engineering, Jining Medical University, China

sensors.[21] Moreover, the background signal could cause serious interference. In recent years, electrochemical sensor based on functionalized nanomaterials have also been reported for the monitoring of Pb^{2+}.[15,22] Considering that these tailor-made materials and biological molecules require skillful design and difficult and long sample-preparation, the prospects for application of these sensors have been limited. In contrast, the QCM biosensor, which is based on the piezoelectric effect and has some advantages, including high sensitivity, low cost, real-time measurement and label-free detection, has been extensively used in various fields, such as environmental monitoring, chemical applications and biotechnology in gas or liquid conditions. The detection principle of QCM is displayed in formula (1),[23]

$$\Delta f = -2\Delta m {f_0}^2/[A(\mu_q\rho_q)^{1/2}]. \quad (1)$$

where Δf is the resonant frequency change (Hz), Δm is the mass change (g), f_0 is the fundamental frequency (Hz) of an AT-cut quartz crystal, A is the area of the electrode (cm^2), μ_q is the shear modulus of the quartz (2.947×10^{11} g cm^{-1} s^{-2}), and ρ_q is the density of the quartz (2.648 g cm^{-3}). Research based on the QCM has been reported for the detection of Bacillus anthracis,[24] Escherichia coli,[25] Campylobacter jejuni,[26] IgG protein[27] and albumin.[28] To improve the performance of biosensors, a signal amplification operation dependent on nanometre materials is generally necessary. AuNPs, with the attractive advantages of their optical properties and high specific surface area, have captured significant attention from researchers in many areas. Hui Boon Teh and coworkers[29] designed a novel, label-free DNAzyme-based QCM-D sensor for monitoring Pb^{2+} with AuNPs as the signal amplification material. And its lowest detectable concentration of Pb^{2+} was 14 nM with good specificity. Nevertheless, a certain environmental condition (37 °C) was indispensable for the whole experiment. Yunfeng Xie *et al.*[30] provided a new strategy for the detection of Pb^{2+}, which was based on the synergistic effect of $Na_2S_2O_3$, 2-mercaptoethanol and Pb^{2+} during the leaching of AuNPs. They indirectly determined the density of Pb^{2+} according to the frequency shifts resulting from the decrease in AuNPs on the surface of QCM. Although, a low detection limit of 30 nM has been realized, the utilization of this sensor would be subject to limitations because of the demand of oxygen.

NMBs, a popular kind of nanoparticle, have been used in the separation and detection of bacteria, viruses and proteins,[31,32] due to their superparamagnetism, high coercivity, small size effect and high magnetization. As far as we know, QCM biosensors combined with NMBs as the amplification strategy have not been built up to now. In this article, we present a novel, simple, highly selective and sensitive method for monitoring Pb^{2+}, which is based on the lead-dependent DNAzyme GR-5 and oligonucleotide functionalized nanomagnetic beads (NMBs-DNA2) on the surface of the QCM. Because NMBs have high mass and superparamagnetism, their participation can greatly improve the sensitivity of the QCM biosensor.

2. Experimental

2.1. Materials and chemicals

The QCM electrodes, with 13.66 mm diameter, 9 MHz resonant frequency and a gold layer which is formed with a diameter size of 6.0 mm on each side, were purchased from Jiaxing Jingkong Electronic Co., Ltd (JJK) in Zhejiang, China. DMSA-modified Fe_3O_4 nanoparticles of a size of 7 nm were offered by Nanjing XFNANO Materials Tech Co., Ltd in Jiangsu, China. Trisodium citrate-modified Fe_3O_4 nanoparticles with a size of 200 nm were purchased from Nanjing Nanoeast Biotech Co., Ltd in Jiangsu, China. Tris(2-carboxyethyl) phosphine hydrochloride (TCEP), 6-mercapto-1-hexano (MCH), 1-ethyl-3(3-dimethylaminopr-opyl) carbod-iimide hydrochloride (EDC) and *N*-hydroxy succinimide (NHS) were all provided by Sigma-Aldrich. GR-5 DNAzyme consists of a catalytic strand and a substrate strand. The synthesis and modification of the oligonucleotides, including a thiol-modified catalytic strand (DNA1) and an amino-modified substrate strand (DNA2), were accomplished by Sangon Biotech. Co., Ltd (Shanghai, China). The sequences were as follows:

Catalytic strand: 5′-SH-$(CH_2)_6$-ACA GAC ATC ATC TCT GAA GTA GCG CCG CCG TAT AGT GAG-3′

Substrate strand: 5′-NH_2-$(CH_2)_6$-CTC ACT ATrA GGA AGA GAT GAT GTC TGT-3′

$Pb(NO_3)_2$ was obtained from Chengdu Kelong Chem. Re. Co., Ltd (Sichuan, China). All other reagents were of analytical grade and used without further purification. During the whole experimental process, ultrapure water generated by the UP water purification system (18.25 MΩ cm, Ulpure, Xi'an, China) was used. The DNA dilute solution was 0.01 M sodium phosphate buffer (PBS-1, PH 7.4) containing 0.05 M NaCl and 0.025 M $MgCl_2$.

2.2. Preparation of NMBs-DNA2

NMBs with a diameter of 200 nm were modified with carboxyl groups. To begin with, 50 mg mL^{-1} EDC and NHS diluted in PBS-1 were added into the NMBs solution in a 0.5 ml tube for 30 min under gentle stirring, in order to active the carboxyls on the NMBs.[33] After that, magnetic separation and washing were carried out according to the literature.[34] Briefly, a magnetic field was applied to the side of the tube. After about 2 min, the supernates were removed carefully with a pipette, and fresh sodium phosphate buffer (0.01 M PBS-2, containing only 0.05 M NaCl) was added. Then the magnetic separation steps mentioned above were repeated three times. Fresh PBS-1 and DNA2 solution were added into the NMBs after the last cleaning, which gave a final concentration of DNA2 and the carboxyl groups on the NMBs of about 2.5 μM and 25 μM, respectively. The mixed solution was incubated at room temperature with gentle stirring. After 4 h, the DNA2 uncombined with NMBs was removed under an external magnetic field and

the same aforementioned magnetic cleaning steps were repeated three times. Of course, the NMBs which have not been bound with DNA2 have also been retained under the magnetic field. They can be rinsed during the subsequent assay due to its non-combining capacity with DNA1. Compared with gold nanoparticles, using NMBs may be more beneficial in this process. Then, the mixed solution was incubated in 0.05 M tris-HCl (PH 7.4) for 15 min and finally stored in 0.025 M tris-acetate (PH 7.2) at 4 °C for subsequent use.

2.3. Preparation of the QCM biosensors

The AT-cut gold-coated quartz crystal sensor was prepared offline, and the detection processes were carried out with a home-made frequency meter. The whole experimental procedure consists of the following four steps. To begin with, the electrode was cleaned with absolute ethyl alcohol, 1 M sodium hydroxide solution and 1 M hydrochloric acid for nearly 2 h, 20 min and 20 min, respectively. Then, the electrode was rinsed thoroughly with ultrapure water and dried under nitrogen. Secondly, DNA1 solution was diluted in a buffer solution (PBS-1) containing 10 mM TCEP to a final concentration of 2 μM and incubated for 1 h at room temperature to avoid disulfide bond formation. The cleaned QCM was treated with 20 μL of DNA1 solution overnight at 4 °C. This was followed by the removal of the unbound DNA1 strands with the buffer solution (PBS-2) and ultrapure water. 20 μL of 10 mM MCH in PBS-1 buffer solution as a blocking buffer was dropped on the QCM gold electrode for 1 h at 4 °C. Finally, after rinsing of the electrode three times, it was further incubated with the prepared NMBs-DNA2 for 1 h at 37 °C. Thus, the NMBs were labeled on the electrode through the hybridization between DNA1 and DNA2.

2.4. The detection of the QCM electrodes

When different concentrations of Pb^{2+} were cast on the electrodes for 2 h, DNA2 was cut into two parts at the 'rA' site, along with the release of NMBs and DNA2. Following rinsing with washing buffer, the electrode was measured with the frequency meter at room temperature. The frequency can be stable in about 2 min after installing the QCM electrode.

3. Results and discussion

3.1. Design of the QCM lead biosensor

The DNAzymes of Pb^{2+} include GR-5 and 8–17 DNAzyme. However, 8–17 DNAzyme is also active for other metal ions, such as Co^{2+} and Zn^{2+}.[35] GR-5 DNAzyme has a higher specificity for Pb^{2+}. The whole process is illustrated in Fig. 1. The catalytic strand and substrate strand were used in the sensor fabrication. The former strand, modified with a thiol group at its 5′-end, was fixed on the QCM surface. Since the mass of DNA is feeble, the two DNA strands alone cannot lead to a big frequency change on the QCM in the presence of Pb^{2+}.[29] Therefore, signal amplification is essential to enhance the sensitivity of the sensor. In our work, the NMBs-DNA2 complex, which consists of DNA2 modified with an amino group and the carboxyl-NMBs, was hybridized with DNA1 to immobilize the NMBs onto the QCM. The presence of NMBs enhanced the mass variation that arose from substrate cleavage in the presence of Pb^{2+}. So the sensitivity of our biosensor was further enhanced. When the electrode was exposed to Pb^{2+}, a bigger frequency change was obtained because of the release of the NMBs-DNA2 complex. At different concentrations of Pb^{2+}, different frequency changes were measured by the frequency meter.

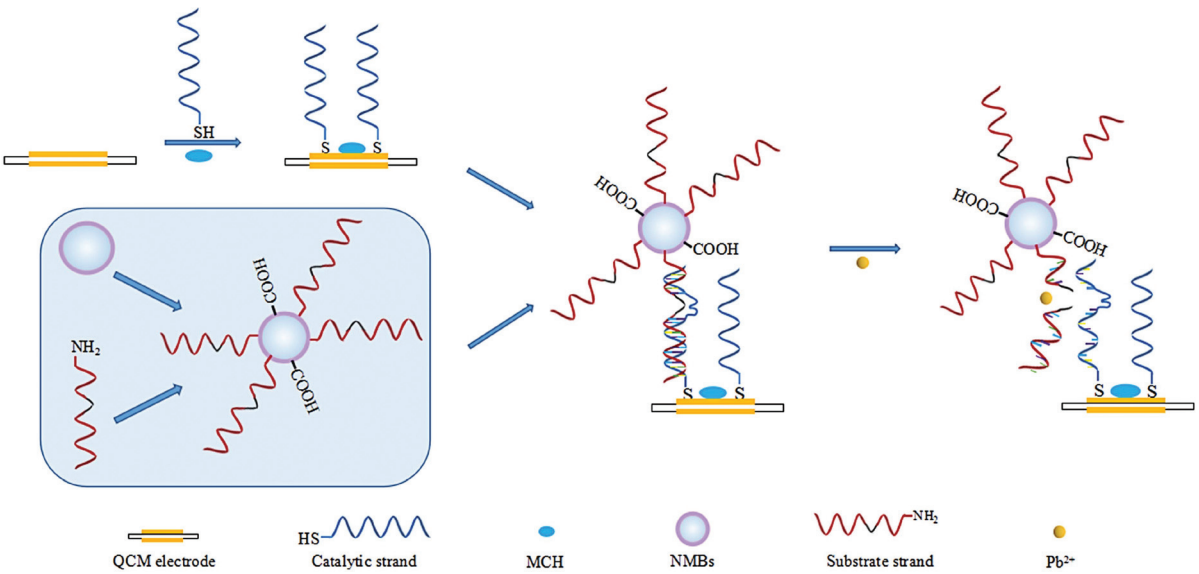

Fig. 1 A schematic view of the preparation of the QCM sensor for the detection of Pb^{2+}.

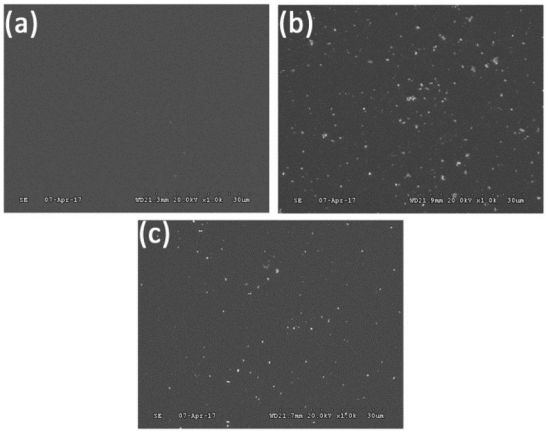

Fig. 2 SEM image of the cleaned QCM (a), electrode after the immobilization of NMBs-DNA2 (b), electrode after the modification of Pb^{2+} (c).

3.2. The characterization of the QCM electrodes

The electrodes were characterized using a scanning electron microscope (SEM) in order to elucidate the modification effect of our method. Fig. 2a–c show the SEM images of a cleaned electrode, an electrode modified with NMBs-DNA2 and an electrode treated with Pb^{2+}, respectively. As can be seen from the images, Fig. 2a displays the smooth surface of the electrode, while plenty of white light spots that signify NMBs can be found in Fig. 2b, which confirms that the NMBs were successfully bonded to the gold surface. In comparison, Fig. 2c indicates that the number of NMBs is less than that in Fig. 2b, which is attributed to the existence of Pb^{2+}. The DNAzyme was cut into two parts at the 'rA' site, and the whole DNA2 fragment was released and the NMBs on these DNA2 fragments also fell off after rinsing with buffer solution. Hence, the results indicate that the fabrication of our biosensor was successful.

3.3. Optimization of experimental conditions

In order to improve the sensitivity of the biosensor, it is necessary to optimize some vital factors, including the concentration of DNA1 and the binding efficiency of NMBs with DNA2. Hence, we discuss the optimal concentration of DNA1 firstly. As shown in Fig. 3, with increasing concentration of DNA1, the variation in frequency increased to a peak value of 38.2 Hz, corresponding to a DNA1 concentration of 2 μM, and then declined. This reduction was probably attributable to the enhancement of the steric hindrance and electrostatic repulsion resulting from the increase in DNA1 on the surface. Thus, 2 μM was chosen as optimal concentration of DNA1. Moreover, the effective combination of NMBs with DNA2 is also very important for the whole assay. So we explored the effect of combination with no NMBs and two kinds of NMBs whose diameters are respectively about 7 nm and 200 nm under the condition of 0.5 μM DNA1. As displayed in Fig. 4a, compared with the results received on the electrode without NMBs, the frequency variations of the NMBs-combined electrodes are both

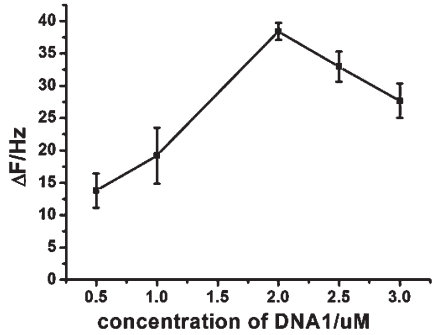

Fig. 3 The fixed efficiency of DNA1 on the QCM electrodes surface.

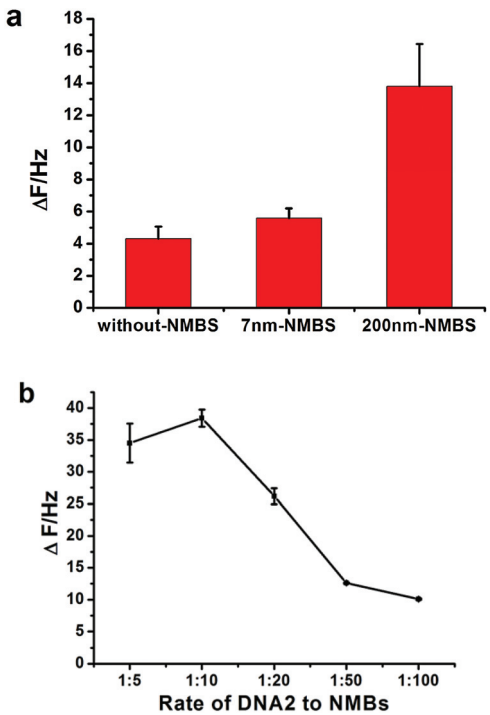

Fig. 4 The effect of nanomagnetic beads with different sizes on the frequency change (a), different concentration ratios of DNA2 to carboxyl group on nanomagnetic beads. DNA2 were 2.5 μM (b).

bigger, which indicates that the amplification of NMBs-DNA2 has been achieved. The reason is that the mass of DNA2 is much less than that of NMBs-DNA2. And the frequency shifts were about 5.57 Hz and 13.79 Hz for 7 nm and 200 nm, respectively. Since the bigger NMBs possess greater mass, the NMBs with a size of 200 nm can result in larger frequency changes. In addition, the number of carboxyl groups on the bigger NMBs would be more than that on the smaller ones, which leads to conjugation with more DNA2 through the combination between carboxyl groups and amino groups. As a consequence, the NMBs can be fixed firmly onto the QCM through the specific binding between DNA2 and DNA1. So, the 200 nm NMBs were selected for our work.

What is more, the concentration of NMBs will affect the joint efficiency between DNA1 and DNA2. Although the concentration of carboxyl groups on NMBs was 2600 μM, only 20–30% of them can be activated under the effect of EDC/NHS. Excessive NMBs could induce their reunion. So it is important to optimize the ratio of DNA2 and NMBs. We presumed that just 20% of carboxyl groups can be activated on the NMBs. And then, we investigated the ratio of the amino concentration which is equivalent to DNA2 to the carboxyl group concentration on the NMBs. As indicated in Fig. 4b, the frequency change reached its peak value when the concentration of carboxyl groups was ten times than that of the amino groups. It is not beneficial for the effective combination of NMBs-DNA2 and DNA1 due to the agglomeration caused by too many NMBs. So, we chose 1 : 10 as the optimal ratio.

3.4. Sensitivity of the QCM biosensor

To study the sensitivity of our method, the QCM electrodes were incubated with different concentrations of Pb^{2+} under optimum conditions for 2 h and the frequency values were recorded after each modification. As shown clearly in Fig. 5a, the frequency variation increased with the rising concentration of Pb^{2+}. The calibration curve showed a good linear correlation between the frequency variations and the logarithm of Pb^{2+} concentration from 1 pM to 50 nM, with a correlation coefficient of 0.99634. We have achieved the detection of 100 nM of Pb^{2+} and found that the result registered a minute change, which is possibly attributable to the limited compound amount of GR-5 DNAzyme and NMBs, so that the shearing effect of Pb^{2+} has been saturated. The detection limit of our biosensor is 0.3 pM, which is lower than that of most other lead sensors, as shown in Table 1. As there is an inductive effect in the equivalent circuit model of QCM, the superparamagnetism of NMBs is probably conducive to strengthening the efficiency of the inductor. So NMBs may have a positive influence on the lower detection limit of the QCM besides their mass. Furthermore, the QCM electrode is packaged into a metal casing which can effectually avoid the interference of dust and airflow. Thus, our method has potential for the real-time monitoring of Pb^{2+} in our daily lives.

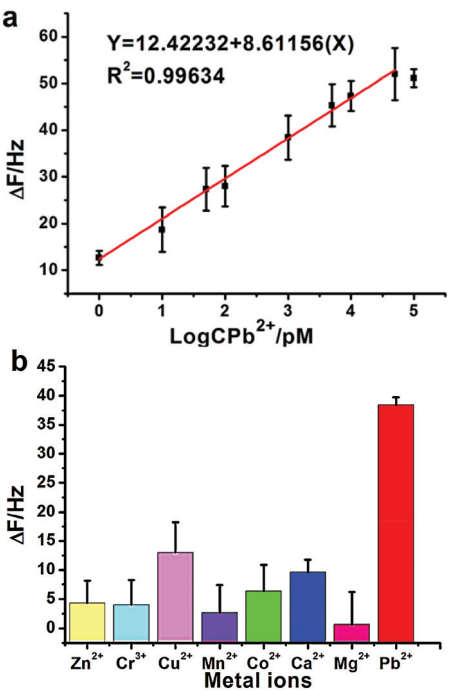

Fig. 5 The calibration curve of the frequency variation for different concentrations of Pb^{2+} (a); specificity of the QCM biosensor towards Pb^{2+} and other metal ions: Zn^{2+}, Cr^{3+}, Cu^{2+}, Mn^{2+}, Co^{2+} and Ca^{2+} and Mg^{2+}; all of these metal ions were 1 nM (b). The error bars represent the standard deviations based on three independent measurements.

Table 1 Comparison of sensitivity of the proposed QCM biosensor with other recently reported sensors

Methods	Detection limit	Linear rage	Ref.
AAS	14.5 nM	48.3 nM–4.83 μM	4
GFAAS	0.386 nM	—	5
MC-ICP-MS	0.483 nM	—	6
Electrochemical	32 pM	0.05–50 nM	14
QCM-D	14 nM	46–3000 nM	29
QCM-AuNPs	30 nM	0.1–10 μM	30
Electrochemical	6.61 nM	10–100 nM	35
Fluorescence	0.4 nM	0.5–500 nM	36
Colorimetric	20 pM	0.05–5 nM	37
Electrochemical	2 pM	5 pM–2 μM	38
QCM-NMBs	0.3 pM	1 pM–50 nM	This work

3.5. Selectivity of the QCM biosensor

The specificity of our sensor was also investigated by comparing Pb^{2+} with other metal ions. 1 nM of Zn^{2+}, Cr^{3+}, Cu^{2+}, Mn^{2+}, Co^{2+}, Ca^{2+}, Mg^{2+} and Pb^{2+} were all measured separately. The results are shown in Fig. 5b. With a uniform concentration, Pb^{2+} caused much higher frequency shifts than those of other metal ions. It is obvious that this sensor has high selectivity.

3.6. Practicability of our biosensor

According to the condition of our laboratory, it is not easy to obtain the polluted water samples detected by international standard testing. So, in order to prove the practicability of our work, we have tested the recovery of the QCM biosensor with different concentrations of Pb^{2+} in drinking water (Wahaha). What we can see from Table 2 is that our method based on an NMBs-enhanced QCM for the detection of Pb^{2+} showed the recovery of three concentrations of lead ions ranging from 90.65% to 103.58%, and the error is acceptable. Thus, this approach shows a useful value for the determination of Pb^{2+}.

Table 2 Results of Wahaha drinking water sample (n = 3)

Sample	Detection	Recovery
10 pM	9.0648 pM	90.65%
100 pM	91.994 pM	91.994%
10 nM	10.358 nM	103.58%

4. Conclusions

In summary, we present a novel amplification method based on NMBs for the detection of Pb^{2+} on the QCM. Considering the advantages of their superparmagnetism and high surface area, NMBs were selected for amplification in this article. Our method simultaneously decreased the disturbance of DNA2 which had not been modified with nanomaterials, enhanced the efficiency and simplified the experimental process. Our work reveals a good linear range from 1 pM to 50 nM of Pb^{2+} and the limit of detection is as low as 0.3 pM, which is much lower than the 72 nM suggested by the EPA. Furthermore, this biosensor also displays an ideal recovery of 97 ± 6% in a drinking water sample (Wahaha) and a good specificity against other metal ions. Certainly, considering the superparamagnetic properties of NMBs, a QCM biosensor combined with NMBs may be applied to detect other metal ions or small molecules and can achieve a lower detection limit than that of already existing methods.

Conflicts of interest

There are no conflicts to declare.

Acknowledgements

This work was supported by Chongqing Research Program of Basic Research and Frontier Technology (cstc2015jcyjS20014), the Visiting Scholar Foundation of Key Laboratory of Biorheological Science and Technology (Chongqing University), Ministry of Education (CQKLBST-2015-005). The authors expressed their gratitude for those supports.

Notes and references

1 L. Xu, H. Yin, W. Ma, L. Wang, H. Kuang and C. Xu, *J. Phys. Chem. B*, 2013, **117**, 14367–14371.
2 W. Chu, Y. Zhang, D. Li, C. J. Barrow, H. Wang and W. Yang, *Biosens. Bioelectron.*, 2015, **67**, 621–624.
3 G. Liang, Y. Man, A. Li, X. Jin, X. Liu and L. Pan, *Microchem. J.*, 2017, **135**, 145–153.
4 R. Ma, W. Van Mol and F. Adams, *Anal. Chim. Acta*, 1994, **285**, 33–43.
5 S.-M. Xiao, J.-R. Chen and Y.-Q. Shen, *Guangpuxue Yu Guangpu Fenxi*, 2006, **26**, 955–958.
6 A. Cocherie and M. Robert, *Chem. Geol.*, 2007, **243**, 90–104.
7 A. Gao, C. X. Tang, X. W. He and X. B. Yin, *Analyst*, 2013, **138**, 263–268.
8 J. Zhang, Y. Tang, L. Teng, M. Lu and D. Tang, *Biosens. Bioelectron.*, 2015, **68**, 232–238.
9 H. Wei, B. Li, J. Li, S. Dong and E. Wang, *Nanotechnology*, 2008, **19**, 95501.
10 L. Zhang, B. Han, T. Li and E. Wang, *Chem. Commun.*, 2011, **47**, 3099–3101.
11 C. B. Swearingen, D. P. Wernette, D. M. Cropek, Y. Lu, J. V. Sweedler and P. W. Bohn, *Anal. Chem.*, 2005, **77**, 442–448.
12 Y. Zhao, Q. Zhang, W. Wang and Y. Jin, *Biosens. Bioelectron.*, 2013, **43**, 231–236.
13 L. Shen, Z. Chen, Y. Li, S. He, S. Xie, X. Xu, Z. Liang, X. Meng, Q. Li, Z. Zhu, M. Li, X. C. Le and Y. Shao, *Anal. Chem.*, 2008, **80**, 6323–6328.
14 B. Zhang, J. Chen, B. Liu and D. Tang, *Biosens. Bioelectron.*, 2015, **69**, 230–234.
15 S. Tang, W. Lu, F. Gu, P. Tong, Z. Yan and L. Zhang, *Electrochim. Acta*, 2014, **134**, 1–7.
16 Q. Zhou, Y. Lin, Y. Lin, Q. Wei, G. Chen and D. Tang, *Biosens. Bioelectron.*, 2016, **78**, 236–243.
17 T. Lan, K. Furuya and Y. Lu, *Chem. Commun.*, 2010, **46**, 3896.
18 H. N. Kim, W. X. Ren, J. S. Kim and J. Yoon, *Chem. Soc. Rev.*, 2012, **41**, 3210–3244.
19 L. Shi, G. Liang, X. Li and X. Liu, *Anal. Methods*, 2012, **4**, 1036.
20 P. Chen, R. Zhang, Q. Jiang, X. Xiong and S. Deng, *J. Biomed. Sci. Eng.*, 2015, **8**, 451–457.
21 C. Liu, C. Huang and H. Chang, *Anal. Chem.*, 2009, **81**, 2383–2387.
22 H. Zhang, B. Jiang, Y. Xiang, J. Su, Y. Chai and R. Yuan, *Biosens. Bioelectron.*, 2011, **28**, 135–138.
23 R. Akter, C. K. Rhee and M. A. Rahman, *Biosens. Bioelectron.*, 2015, **66**, 539–546.
24 R. Z. Hao, H. Bin Song, G. M. Zuo, R. F. Yang, H. P. Wei, D. B. Wang, Z. Q. Cui, Z. P. Zhang, Z. X. Cheng and X. E. Zhang, *Biosens. Bioelectron.*, 2011, **26**, 3398–3404.
25 X. Mao, L. Yang, X.-L. Su and Y. Li, *Biosens. Bioelectron.*, 2006, **21**, 1178–1185.
26 N. A. Masdor, Z. Altintas and I. E. Tothill, *Biosens. Bioelectron.*, 2016, **78**, 328–336.
27 H. Ogi, K. Motohisa, K. Hatanaka, T. Ohmori, M. Hirao and M. Nishiyama, *Biosens. Bioelectron.*, 2007, **22**, 3238–3242.
28 T. Y. Lin, C. H. Hu and T. C. Chou, *Biosens. Bioelectron.*, 2004, **20**, 75–81.
29 H. B. Teh, H. Li and F. Yau, *Analyst*, 2014, **139**, 5–6.
30 Y. Xie, Y. Jin, Y. Huang, G. Liu and R. Zhao, *Microchim. Acta*, 2014, **181**, 1521–1527.
31 Z. Yang, C. Lei and Y. Zhou, Detection of C-reactive protein based on a Dynabeads-labeled sandwich immunoassay by using a GMI biosensor, 9th International Conference on Bioinformatics and Biomedical Engineering iCBBE 2015, 2015.
32 Z. Yang, Y. Liu, C. Lei, X. c. Sun and Y. Zhou, *Microchim. Acta*, 2015, **182**, 2411–2417.
33 J. Gu, X. Lu and H. Ju, *Electroanalysis*, 2002, **14**, 949–954.
34 Y. Pan, M. Guo, Z. Nie, Y. Huang, C. Pan, K. Zeng, Y. Zhang and S. Yao, *Biosens. Bioelectron.*, 2010, **25**, 1609–1614.
35 H. Cui, X. Xiong, B. Gao, Z. Chen, Y. Luo, F. He, S. Deng and L. Chen, *Electroanalysis*, 2016, **28**, 2000–2006.
36 W. Wang, Y. Jin, Y. Zhao, X. Yue and C. Zhang, *Biosens. Bioelectron.*, 2013, **41**, 137–142.
37 W. Yun, D. Cai, J. Jiang, P. Zhao, Y. Huang and G. Sang, *Biosens. Bioelectron.*, 2016, **80**, 187–193.
38 S. Ge, K. Wu, Y. Zhang, M. Yan and J. Yu, *Biosens. Bioelectron.*, 2016, **80**, 215–221.

